

Radiation-hard detectors for very high luminosity colliders

Andrea Candelori
(INFN Padova)

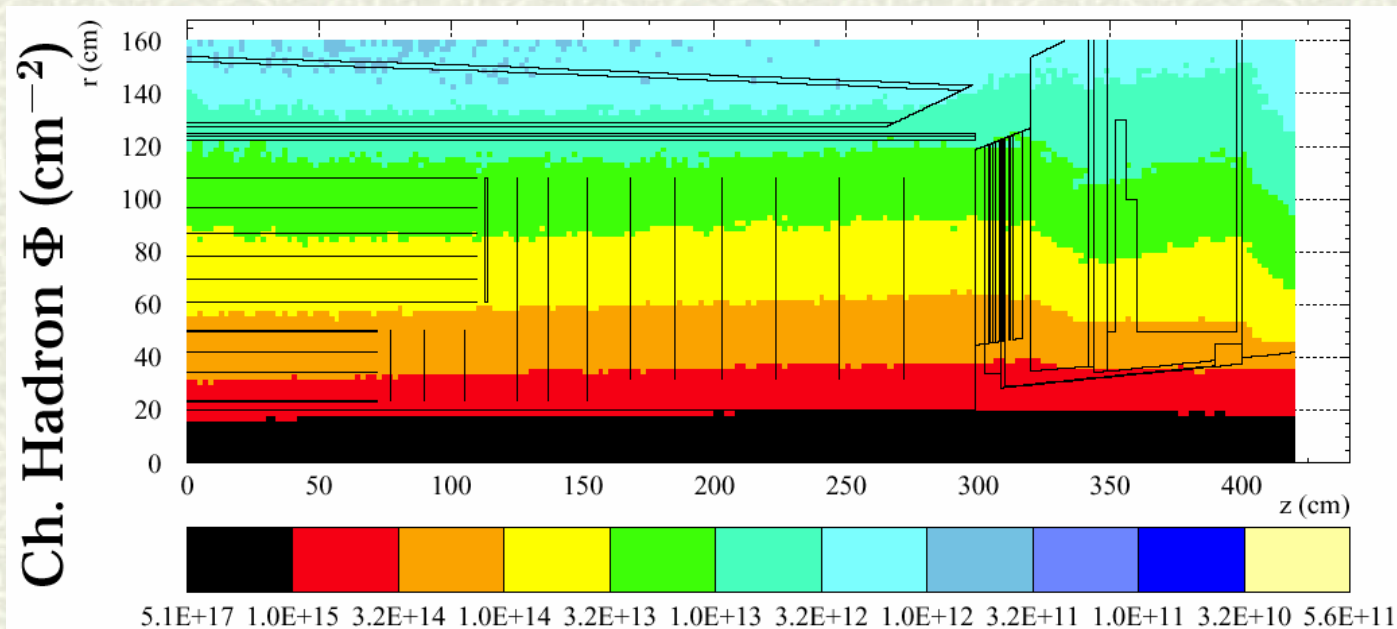
On behalf of the RD50 Collaboration
(<http://rd50.web.cern.ch/rd50/>)

- Motivations: the LHC upgrade
- The RD50 Collaboration
- Radiation effects in silicon detectors
- Leakage current density increase
- Oxygen and effective doping concentrations
- Czochralski and Magnetic Czochralski silicon
- Thin detectors: thinned and epitaxial
- 3-D, Semi 3-D and Stripixel detectors
- p-type substrate
- CCE simulations for pixel detectors
- CCE in SiC and GaN
- Summary

LHC upgrade: from LHC to Super-LHC

(M. Hutinen: "Radiation issues for S-LHC", S-LHC Electronics Workshop, 26/2/04, CERN
O. Bruning: "Accelerator upgrades for S-LHC", S-LHC Electronics Workshop, 26/2/04, CERN)

	LHC	=>	S-LHC
Proton Energy:	7 TeV	=>	15 TeV
Collision rate:	40 MHz	=>	80 MHz
Peak luminosity:	$10^{34} \text{ cm}^{-2} \times \text{s}^{-1}$	=>	$10^{35} \text{ cm}^{-2} \times \text{s}^{-1}$
Integrated luminosity:	500 fb ⁻¹	=>	2500 fb ⁻¹



Approach for tracker upgrade

Radial distances of the actual CMS tracker		Expected S-LHC fluence for fast hadrons	Expected S-LHC dose
Pixel:	4 cm	=> $1.6 \cdot 10^{16} \text{ cm}^{-2}$	420 Mrad
	11 cm	=> $2.3 \cdot 10^{15} \text{ cm}^{-2}$	94 Mrad
Microstrip:	22 cm	=> $8 \cdot 10^{14} \text{ cm}^{-2}$	35 Mrad
	115 cm	=> $1 \cdot 10^{14} \text{ cm}^{-2}$	9 Mrad

The current detector technologies can operate up to $\approx 10^{15} \text{ cm}^{-2}$!

Region	Approach for the tracker upgrade
R < 20 cm	=> R&D required
20 cm < R < 60 cm	=> Improving pixel technology
R > 60 cm	=> Improving microstrip technology

(see talk by R. Horisberger on CMS upgrade for S-LHC, yesterday)

The RD50 Collaboration

RD50: Development of Radiation Hard Semiconductor Devices for High Luminosity Colliders

1. Formed in November 2001
2. Approved by CERN in June 2002

Main objective:

Development of ultra-radiation hard semiconductor detectors for the luminosity upgrade of LHC to $10^{35} \text{ cm}^{-2}\text{s}^{-1}$ (S-LHC).

Challenges:

- Radiation hardness up to fluences of 10^{16} cm^{-2} required;
- Fast signal collection (10 ns bunch crossing);
- Low mass (reducing multiple scattering close to interaction point);
- Cost effectiveness.

Presently 280 Members from 55 Institutes

Belgium (Louvain), **Canada** (Montreal), **Czech Republic** (Prague (2x)), **Finland** (Helsinki (2x), Oulu), **Germany** (Berlin, Dortmund, Erfurt, Halle, Hamburg, Karlsruhe), **Greece** (Athens), **Israel** (Tel Aviv), **Italy** (Bari, Bologna, Florence, Milano, Modena, Padova, Perugia, Pisa, Trento, Trieste, Turin), **Lithuania** (Vilnius), **Norway** (Oslo (2x)), **Poland** (Warsaw), **Romania** (Bucharest (2x)), **Russia** (Moscow (2x), St.Petersburg), **Slovenia** (Ljubljana), **Spain** (Barcelona, Valencia), **Sweden** (Lund) **Switzerland** (CERN, PSI), **Ukraine** (Kiev), **United Kingdom** (Exeter, Glasgow, Lancaster, Liverpool, London, Sheffield, University of Surrey), **USA** (Fermilab, Purdue University, Rutgers University, Syracuse University, BNL, University of New Mexico)

Radiation effects in silicon detectors

I) Increase of the leakage current:

Increase of the shot noise: $F(\omega)=qI/\pi$

Decrease of the S/N ratio

Increase of power dissipation: $P=V \times I$

Increase of voltage drop on bias resistors: $\Delta V=R \times I$

II) Variation of the depletion voltage (V_{dep}):

$V_{\text{dep}} > V_{\text{breakdown}}$: the detector cannot operate fully depleted

Decrease of the charge collection efficiency

Decrease of the S/N ratio

III) Charge trapping:

Decrease of trapping time constant and mean free path

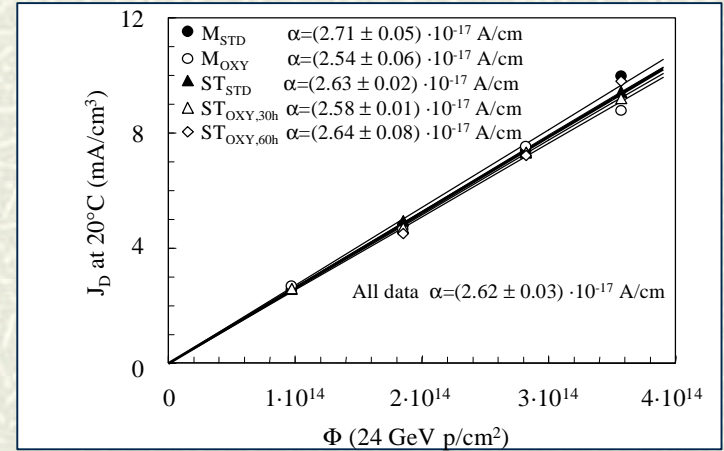
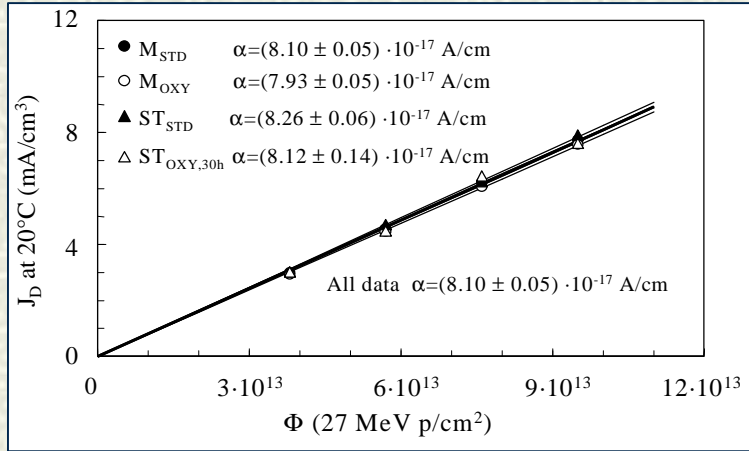
Decrease of the charge collection efficiency

Decrease of the S/N ratio

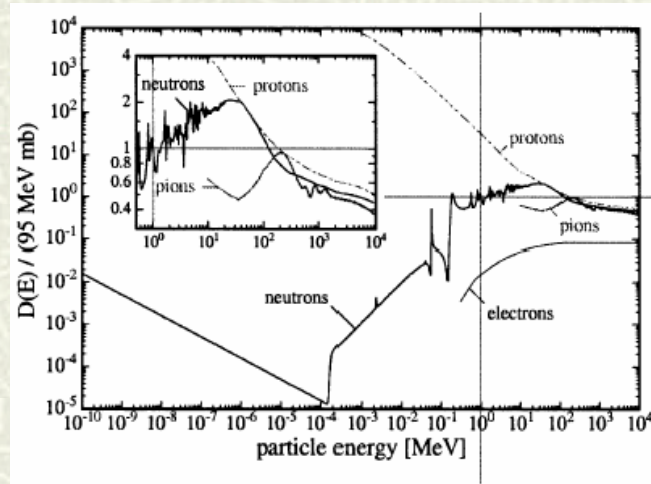
Leakage current density increase

- The leakage current density (**J**) linearly increases with the particle fluence (**F**):

$$J = a \cdot F$$



- The **a** parameter scales with the Non Ionizing Energy Loss (NIEL) of the impinging radiation.

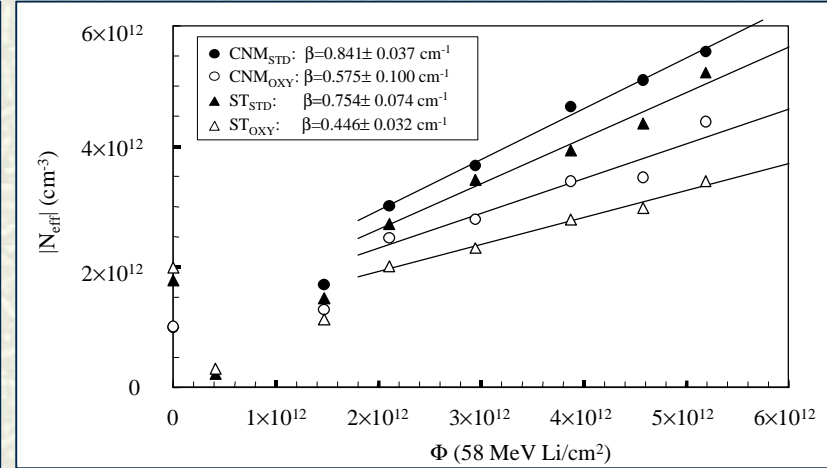
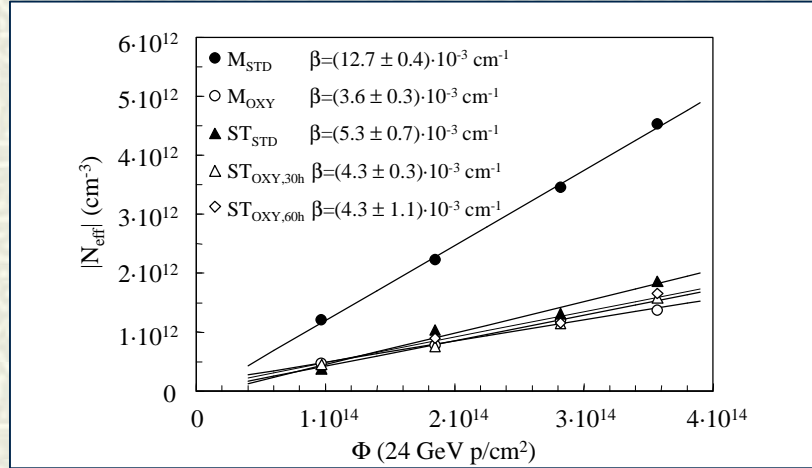


- Possible approach for limiting the leakage current density (**J**): only by decreasing the operating temperature (**T**).
(**J** scales by a factor ≈ 2 every 7.5 K).

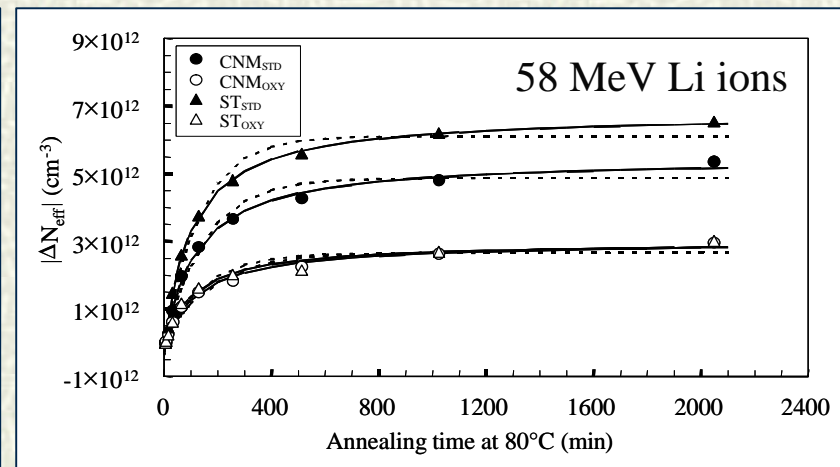
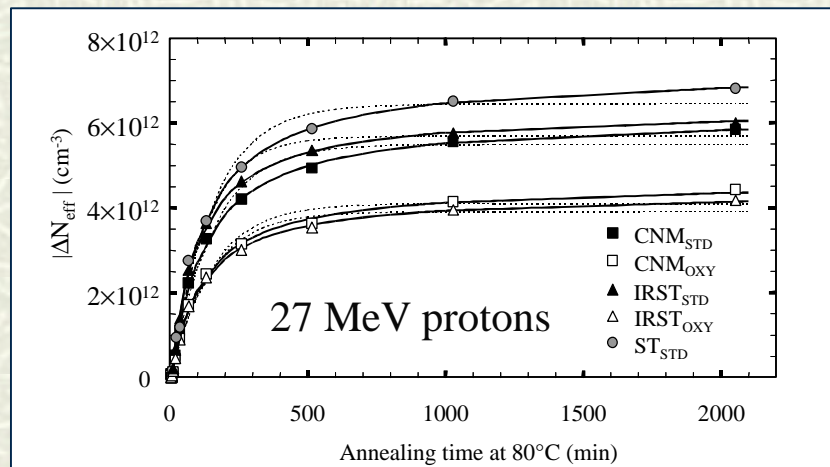
$$J(T_R) = J(T) \left(\frac{T_R}{T} \right)^2 \exp \left(- \frac{E}{2k_B} \left[\frac{1}{T_R} - \frac{1}{T} \right] \right)$$

Oxygen and effective doping concentration (N_{eff})

1. In n-type silicon, radiation induced **donor removal** and **deep acceptor generation** causes the **Space Charge Sign Inversion (SCSI)** effect : the effective doping concentration (N_{eff}), which is initially positive **becomes negative**.
 After SCSI the $|N_{\text{eff}}| \propto V_{\text{dep}}$ increase is mitigated for charged hadrons and ions (not for neutrons) in **Diffusion Oxygenated Float Zone (DOFZ) silicon**, where $[O] > 10^{17} \text{ cm}^{-3}$ in the substrate.



2. After ≈ 20 days at RT since irradiation, $|N_{\text{eff}}| \propto V_{\text{dep}}$ reaches a minimum and **starts to increase** up to saturation (**reverse annealing**).
 The **reverse annealing amplitude** is decreased for charged hadrons and ions (not for neutrons) in **DOFZ Si**, where $[O] > 10^{17} \text{ cm}^{-3}$.



Czochralski (CZ) and Magnetic Czochralski (MCZ) silicon

Advantages:

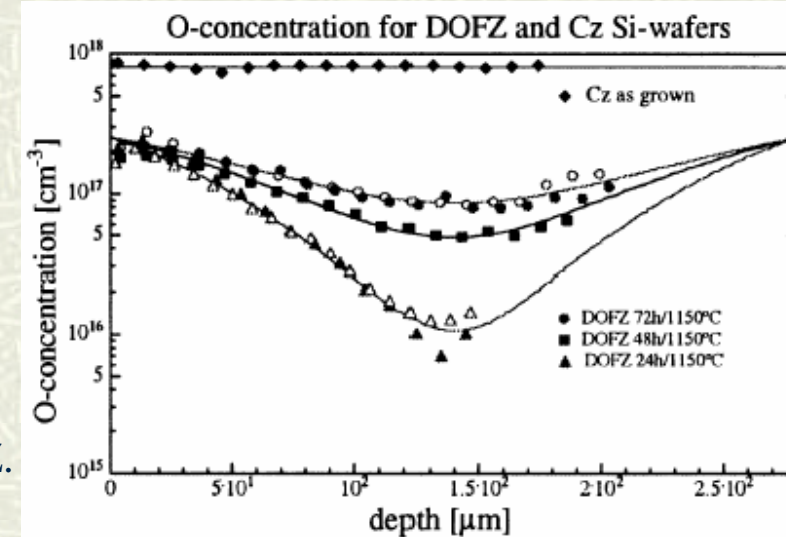
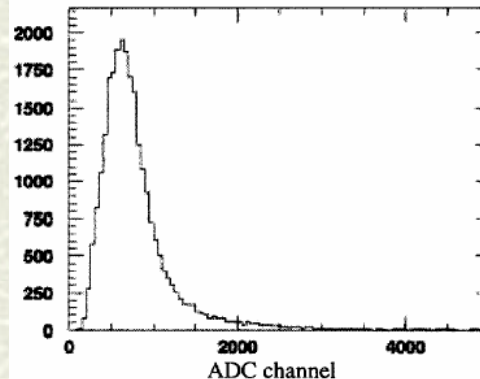
1. **Intrinsic higher oxygen concentration** in **CZ** ($[O] \approx 8-10 \times 10^{17} \text{ cm}^{-3}$) and **MCZ** ($[O] \approx 4-10 \times 10^{17} \text{ cm}^{-3}$) than Float Zone (**FZ**, $[O] < 4 \times 10^{16} \text{ cm}^{-3}$) or Diffusion Oxygenated FZ (**DOFZ**, $[O] \approx 1-4 \times 10^{17} \text{ cm}^{-3}$) Si.
2. No extra process needed for substrate oxygenation.
3. High resistivity ($\approx 1-2 \text{ k}\Omega \times \text{cm}$) p- or n-type **CZ** and **MCZ** wafers **commercially available**.
4. **CZ** and **MCZ** wafers have **higher diameters** (300 mm) than **FZ** and **DOFZ** (150 mm).

Attention has to be considered for avoiding **thermal donor activation** (V_{dep} increase) during processing steps at 450 °C for n-type CZ and MCZ.

Test beam results:

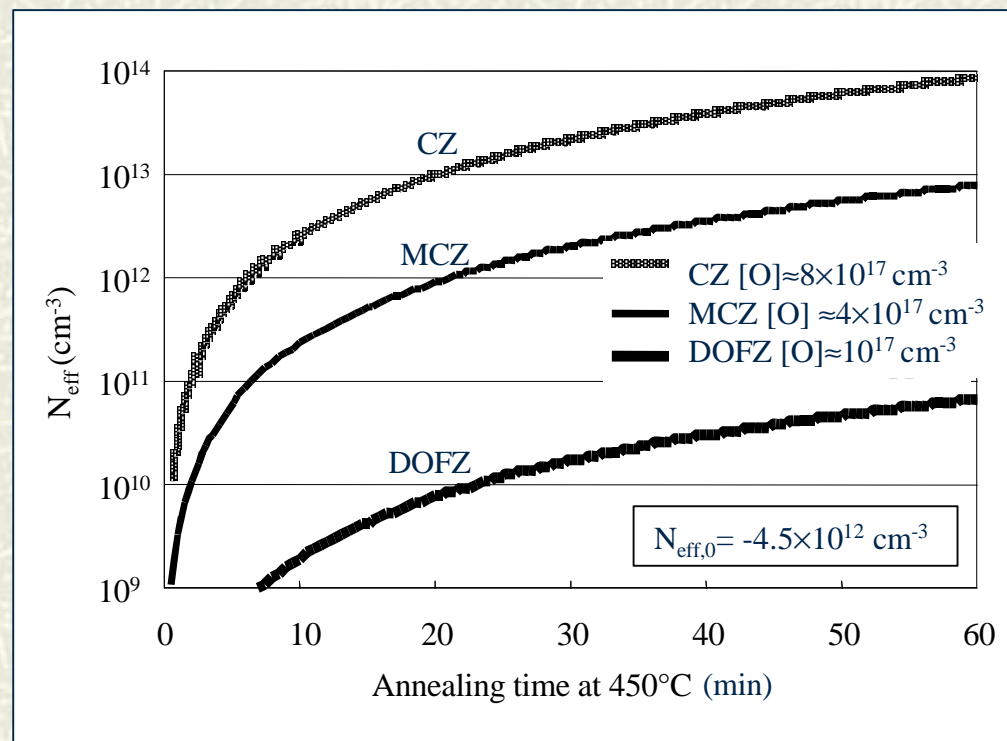
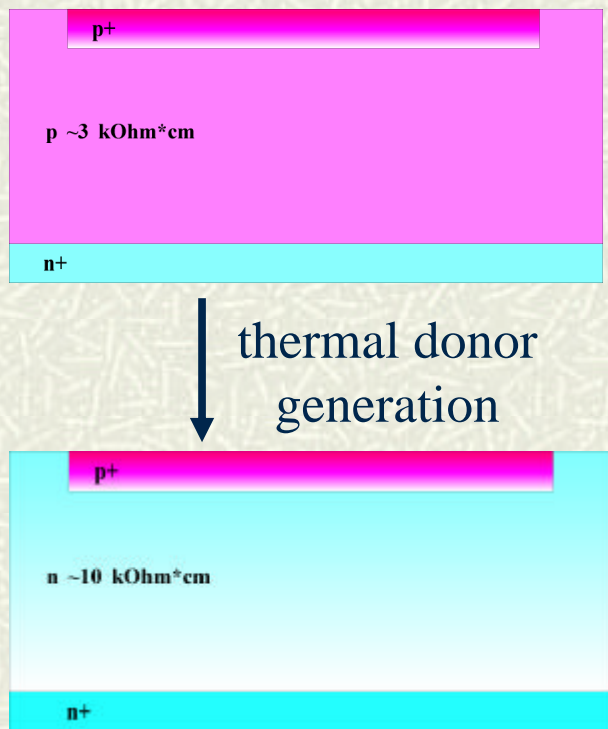
MCZ microstrip detector prototype (AC coupled, with 1024 strips, 6 cm long, $w=10 \mu\text{m}$, $p=50 \mu\text{m}$) has been tested by 225 GeV muon beam at CERN with AV1 chips (resolution $10 \mu\text{m}$ and $S/N=10$).

(E. Tuominen et al., Nuclear Physics B, Proc. Suppl. 125 (2003) 175)



Magnetic Czochralski (MCZ) silicon: thermal donor generation

[O] $\approx 4 \times 10^{17} \text{ cm}^{-3}$ in MCZ silicon is suitable to take advantage of thermal donor generation at 450 °C for processing n-type detectors starting from p-type MCZ substrates.



$$N_{\text{TD}} = \left(\frac{a}{b} \right) (C_{\text{io}})^{\chi} \frac{1}{|N_{\text{d}} - N_{\text{A}}|^2} \left(1 - e^{-b \times D_{\text{i}} \times C_{\text{io}} \times t} \right)$$

N_{DT} is the thermal donor density;
a and b are experimental parameters.

C_{io} is the concentration of interstitial oxygen in silicon;

χ is a constant ($2 < \chi < 3$);

$|N_{\text{d}} - N_{\text{A}}|$ is the free carrier concentration;

D_{i} is the diffusion constant of interstitial oxygen;

t is the time at a given temperature;

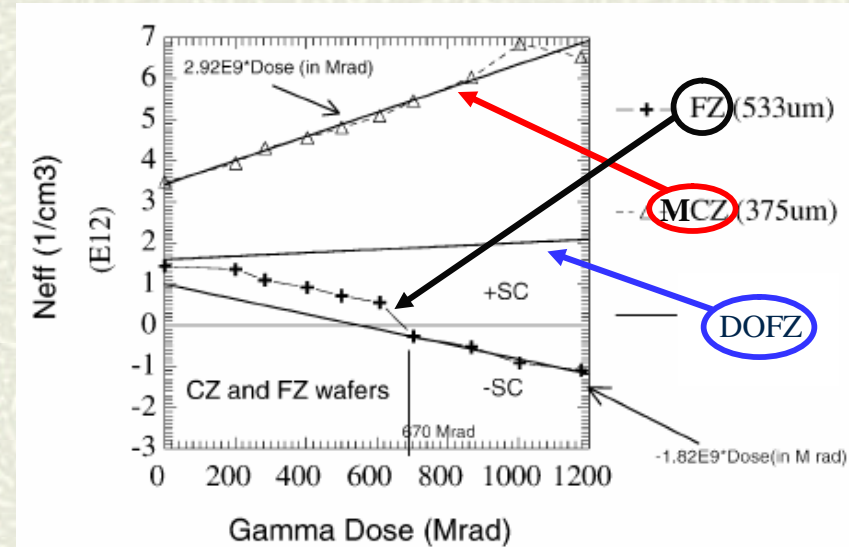
(J. Harkonen et al., 4th RD50 Workshop, <http://rd50.web.cern.ch/rd50/4th-workshop/>)

Magnetic Czochralski (MCZ) silicon: radiation hardness

(Z. Li et al., IEEE TNS 51 (2004) 1901)

⁶⁰Co g-ray irradiation

- SCSI for **FZ** Si,
 $N_{\text{eff}} < 0$ due to deep acceptor generation.
- No SCSI for **MCZ** and **DOFZ** Si,
 N_{eff} increases due to thermal donor activation.



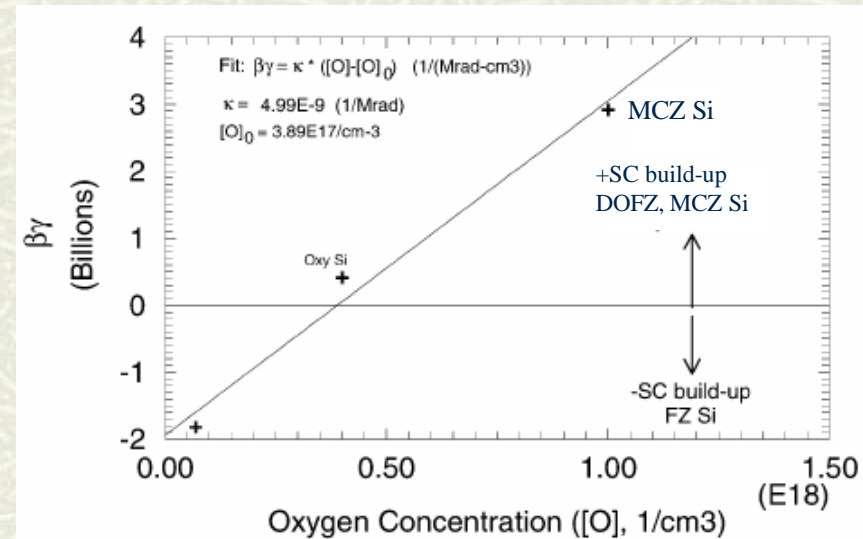
Model for space charge build up in g-irradiated Si

- N_{eff} linearly increases with radiation Dose

$$N_{\text{eff}} = N_{\text{eff},0} + b_g([\text{O}]) \times \text{Dose}$$
- b_g linearly depends on the substrate oxygen concentration

$$b_g = m \times [\text{O}] + q$$

with $m = 4.99 \times 10^{-9} \text{ Mrad}^{-1}$
 $q = 1.94 \times 10^9 \text{ Mrad}^{-1} \times \text{cm}^{-3}$

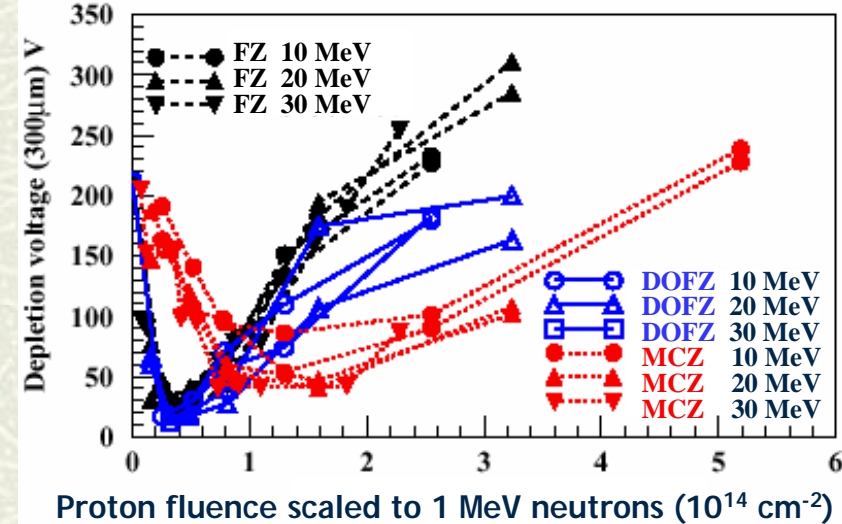


Magnetic Czochralski (MCZ) silicon: radiation hardness

(J. Harkonen et al., NIM A 518 (2004) 346; Z. Li et al., IEEE TNS 51 (2004) 1901)

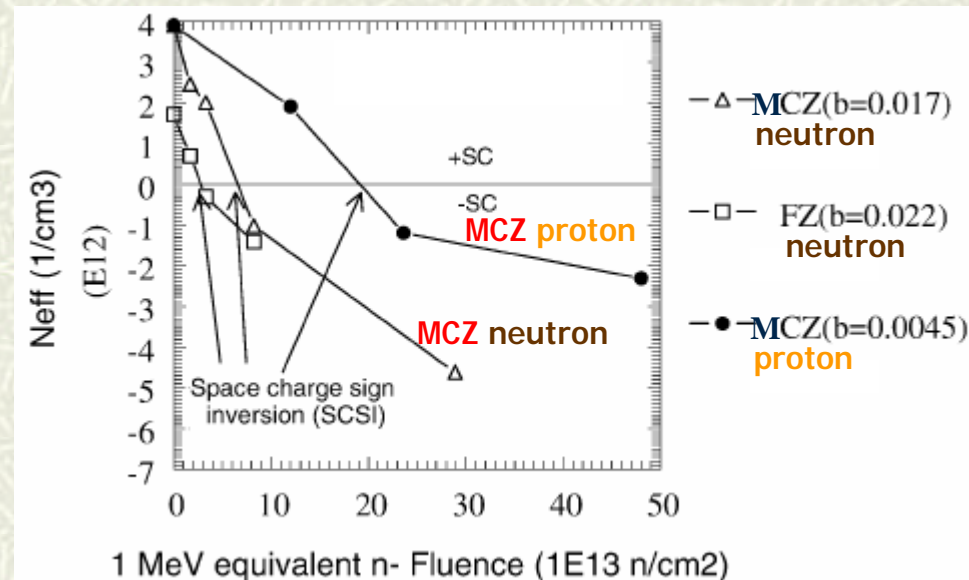
Low energy proton irradiation

1. SCSI occurs in **FZ**, **DOFZ** and **MCZ** Si.
2. **MCZ** detectors present a **lower V_{dep} variation rate** after SCSI than **FZ** and **DOFZ** devices.
3. Oxygen mitigates deep acceptor formation during proton irradiation.



Proton (p) and neutron (n) irradiations

The positive effect of high [O] on $|N_{eff}| \propto V_{dep}$ is strongly reduced when detectors are irradiated by neutrons.



Positive effect of substrate oxygen: microscopic

General microscopic considerations

1) formation of vacancy (V) related defects such as: VO (neutral at RT) or $VO+V=V_2O$ and V_2 related defects (deep acceptors) are competitive processes: VO is enhanced by "high" [O]:

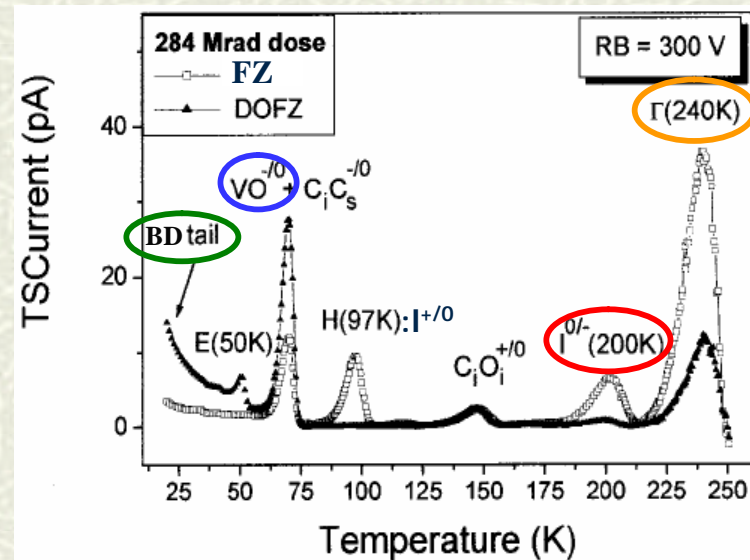
- a. **g-rays**: point defects (i.e., interstitial I and vacancies V) in DOFZ, MCZ and CZ, $[O] \gg [V]$: VO enhanced, V_2O and/or V_2 related defects suppressed
- b. **Neutrons**: clusters (i.e., high defect density regions) in DOFZ, MCZ and CZ, $[O] \ll [V]$: V_2O and/or V_2 related defects present;
- c. **Protons**: point defects and clusters: intermediate condition.

2) Thermal donor activation during irradiation is characteristic for high [O].

^{60}Co g-ray irradiation of FZ and DOFZ silicon

(I. Pintilie et al., NIM A 514 (2003) 18)

Type	I defect	Γ defect	BD center	VO
Energy level	$E_C-0.54$ eV	$E_V+0.68$ eV	$E_C-0.225$ eV	$E_C-0.17$ eV
Effect on N_{eff}	Yes (85% in FZ)	Yes (10% in FZ)	Yes (Compensates Γ and I in DOFZ)	Yes, indirectly: VO is neutral at RT, but VO is a competitive process with V_2O or V_2 related defects and VO is enhanced by high [O].
Effect on I_{leak}	Yes	Yes	No	No
FZ silicon	Present	Present	Absent	Present
DOFZ silicon	Reduced	Reduced	Enhanced with [O]	Enhanced with [O]
Dose dependence	Quadratic \rightarrow Second order defect	Linear	Over linear	-----
Microscopic	$VO+V=V_2O?$	-----	TDD2?	VO

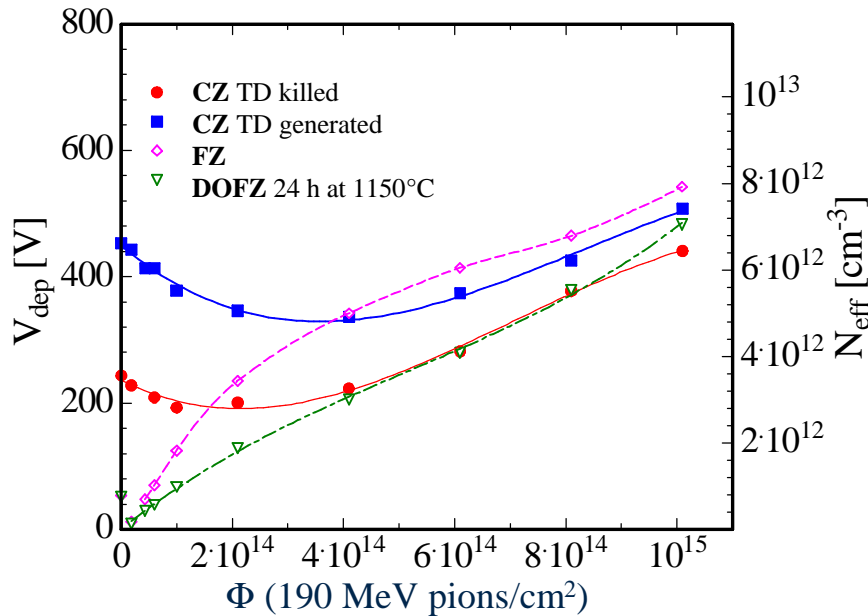


E. V. Monakhov et al. in Phys. Rev. B 68 233203 (2003), investigating the V_2 isothermal annealing at 250 °C by DLTS, proposed that the X center ($E_C-0.47$ eV), whose density linearly depends on [O], observed after that V_2 has been annealed out, is $V_2+O=V_2O$.

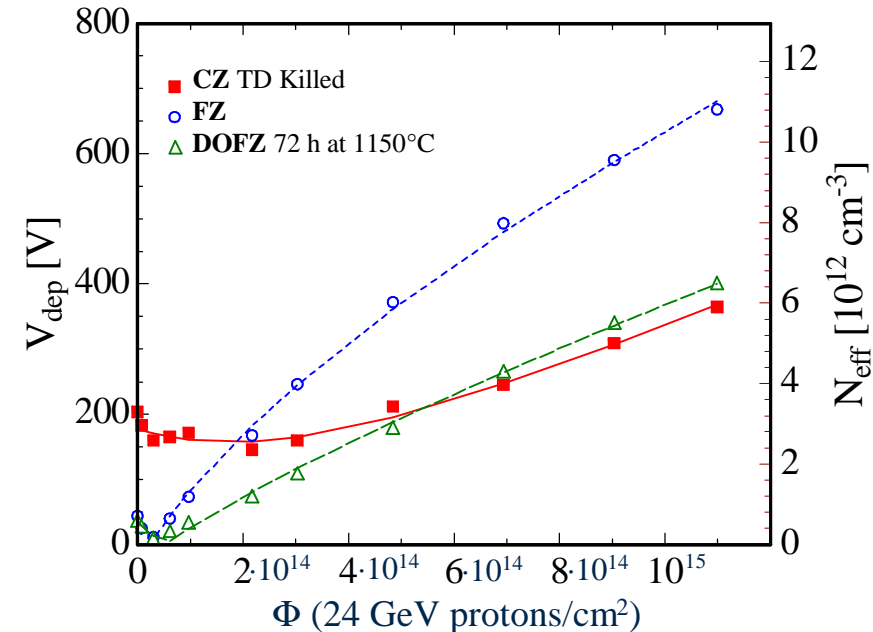
Czochralski (CZ) silicon: radiation hardness

(E. Fretwurst et al., 3rd RD50 Workshop, <http://rd50.web.cern.ch/rd50/3rd-workshop/>)

190 MeV pions



24 GeV protons



- 1) SCSI in **FZ** and **DOFZ** after high energy pion or proton irradiation:
the linear V_{dep} increase for **FZ** and **DOFZ** at high fluences is due to **predominant acceptor generation** (low [O]).
- 2) No SCSI in **CZ** after high energy pion or proton irradiation:
the linear V_{dep} increase for **CZ** at high fluences is due to **predominant donor generation** (high ([O])).
- 3) The linear V_{dep} increase rate at high fluences is lower for **CZ** than for **FZ** and **DOFZ**.

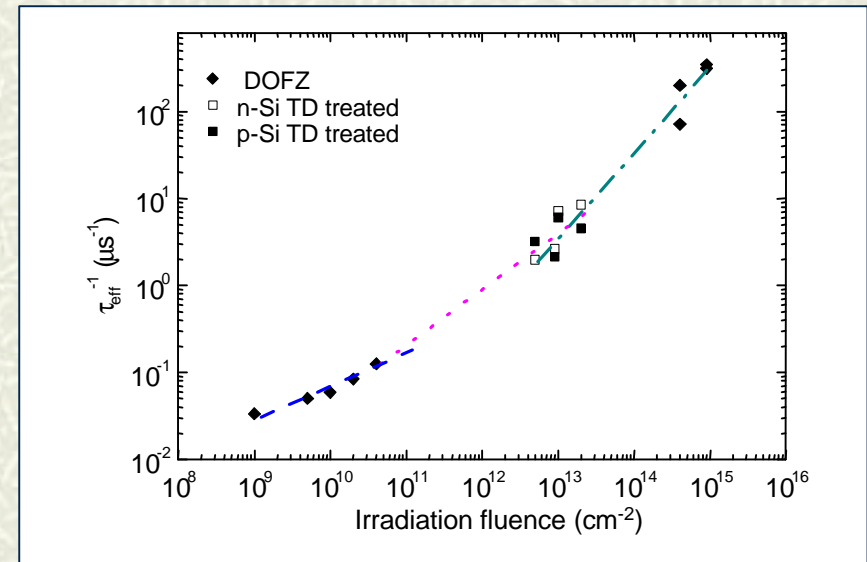
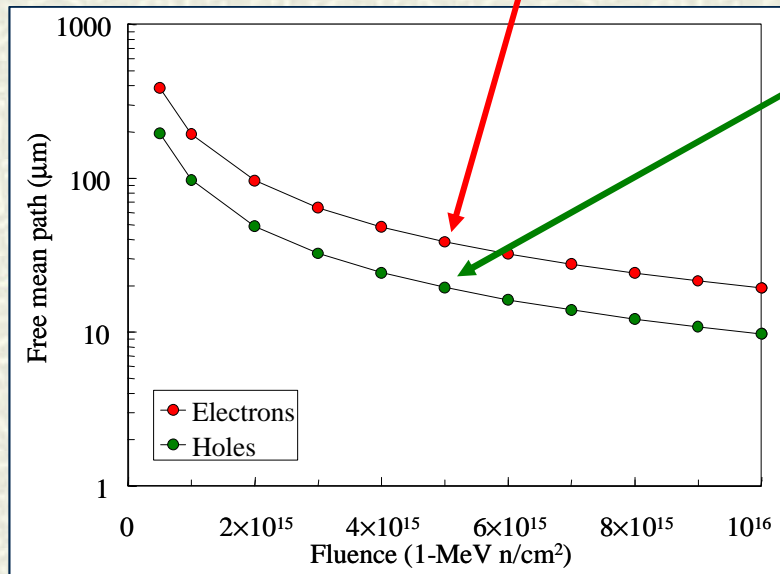
Thin detectors

Why thin detectors?

1. Smaller leakage current: $I_{\text{leak}} \propto W$
2. Smaller depletion voltage: $V_{\text{dep}} = qW^2 N_{\text{eff}} / 2\epsilon \propto W^2$
3. At S-LHC fluences, **charge collection** for planar detectors is **limited by carrier mean free path**, not by the $W \approx 280\text{-}300 \mu\text{m}$ detector thickness

Example.

The trapping time constant (τ) rapidly decreases with fluence ($\Phi_{1\text{-MeV n}}$): $1/\tau_{e,h} = \beta_{e,h} \times \Phi_{1\text{-MeV n}}$
 with $\beta_e = 5.7 \times 10^{-16} \text{ cm}^2/\text{ns}$, $\beta_h = 7.7 \times 10^{-16} \text{ cm}^2/\text{ns}$.
 At $F_{1\text{-MeV n}} = 5 \cdot 10^{15} \text{ cm}^{-2}$ the **carrier mean free path** ($L = v \times \tau$) even at the saturated carrier velocity ($v_{\text{sat,e}} = 1.1 \times 10^7 \text{ cm/s}$, $v_{\text{sat,h}} = 7.5 \times 10^6 \text{ cm/s}$) reduces to $L_e = 40 \mu\text{m}$ for electrons and $L_h = 20 \mu\text{m}$ for holes.

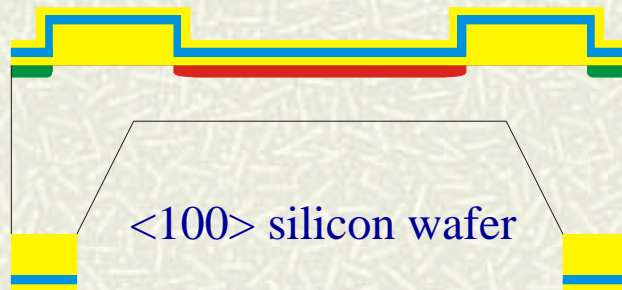


(J.Vaitkus et al., IWORID-6, July 2004, Glasgow)

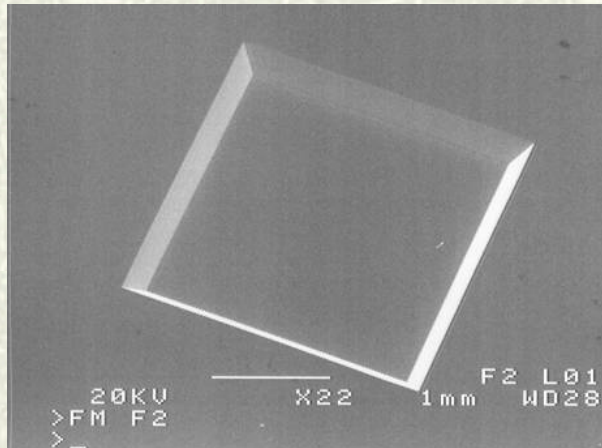
Thin detectors: FZ thinned devices ($W=50 \mu\text{m}$)

ITC-IRST, Trento

(E. Ronchin et al., NIM A 530 (2004) 134)



1. Tetra Methyl Ammonium Hydroxide (TMAH) etching from back.
2. Phosphorous deposition and diffusion from back.
3. Metal deposition from back.



SEM: back view of a thinned device

Areas: $1 \text{ mm}^2 - 20 \text{ mm}^2$ and $I < 1 \text{ nA/cm}^2$ at 20 V

Semiconductor Detector Laboratory, MPI, Munich

(L. Andricek et al., 1st ECFA Workshop, Montpellier, November 2003)

a) oxidation and back side implant of top wafer



b) wafer bonding and grinding/polishing of top wafer

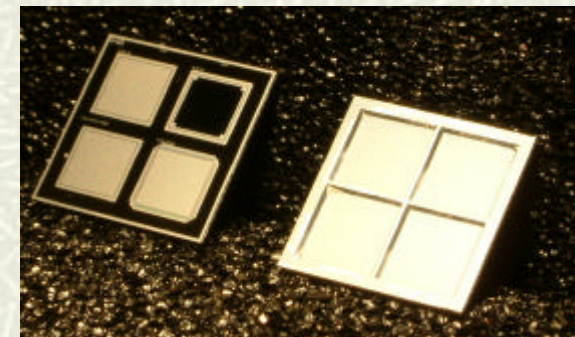
c) process → passivation



open backside passivation



d) anisotropic deep etching opens "windows" in handle wafer



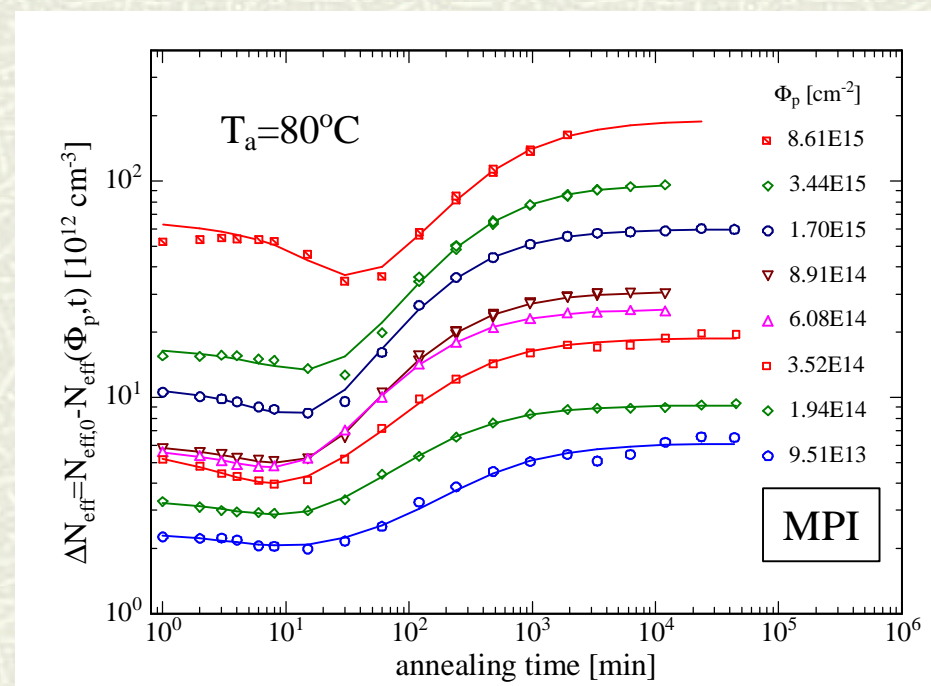
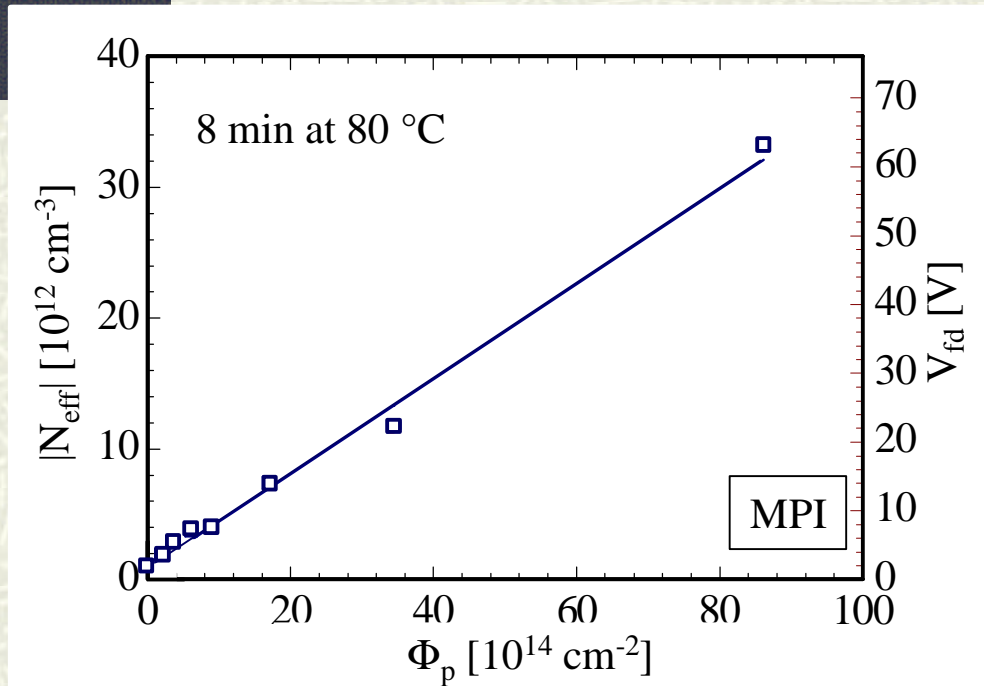
Photograph: front (left) and back (right) view of thinned devices

Area: 10 mm^2 and $I < 1 \text{ nA/cm}^2$ at 20 V

MPI thinned devices ($W=50 \mu\text{m}$): radiation hardness

(E. Fretwurst et al., 4th RD50 Workshop, <http://rd50.web.cern.ch/rd50/4th-workshop>)

20 GeV proton irradiation: $\Phi_p=9.5 \times 10^{13}-8.6 \times 10^{15} \text{ cm}^{-2}$



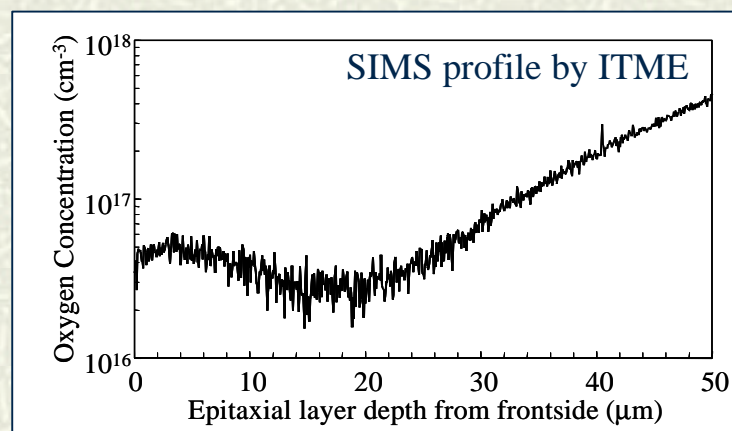
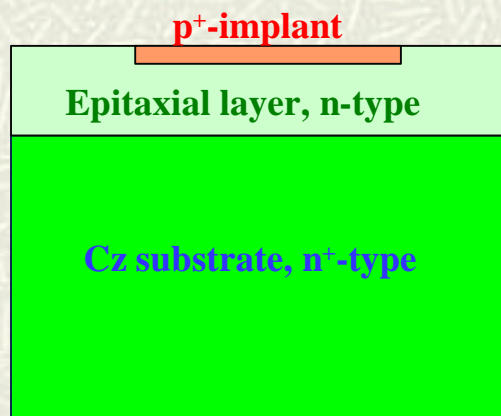
1. $b = D|N_{\text{eff}}| / DF_p = 3.6 \cdot 10^{-3} \text{ cm}^{-1}$ comparable with DOFZ.
2. $V_{\text{dep}} \gg 64 \text{ V}$ for $W=50 \mu\text{m}$ at $F_{\text{max}}=8.6 \cdot 10^{15} \text{ cm}^{-2}$:
 - Ⓜ $V_{\text{dep}} \gg 2300 \text{ V}$ for $W=300 \mu\text{m}$ at $F_{\text{max}}=8.6 \cdot 10^{15} \text{ cm}^{-2}$;
 - Ⓜ $W < 300 \mu\text{m}$ are required at S-LHC.

1. **Stable damage component.**
2. **Short-term component (positive on V_{dep}).**
3. **Long term component: reverse annealing (negative on V_{dep}).**
4. **SCSI reached** before $F_{\text{min}} = 9.5 \cdot 10^{13} \text{ p/cm}^2$.

Thin detectors: epitaxial layer ($W=50\ \mu\text{m}$) on CZ substrate

(Hamburg Group, NIM A 515 (2003) 665)

1. Starting material: **low resistivity** ($\rho < 0.02\ \Omega\cdot\text{cm}$) **300 mm thick Czochralski (CZ) silicon substrate** doped by Sb donors.
2. A thin (**50 nm**) low resistivity ($r=50\ \text{W}\times\text{cm}$), **epitaxial silicon layer** doped by P donors has been grown by ITME (Warsaw, Poland) on the CZ substrate forming a simple $n\text{-}n^+$ structure.
3. p^+ - n junction formed by **B implantation** on the epitaxial layer in a standard way using planar technology by CiS (Institute for Micro Sensors gGmbH, Erfurt, Germany) in order to obtain $p^+\text{-}n\text{-}n^+$ silicon detectors.
4. The detector active thickness is that of the epitaxial layer.



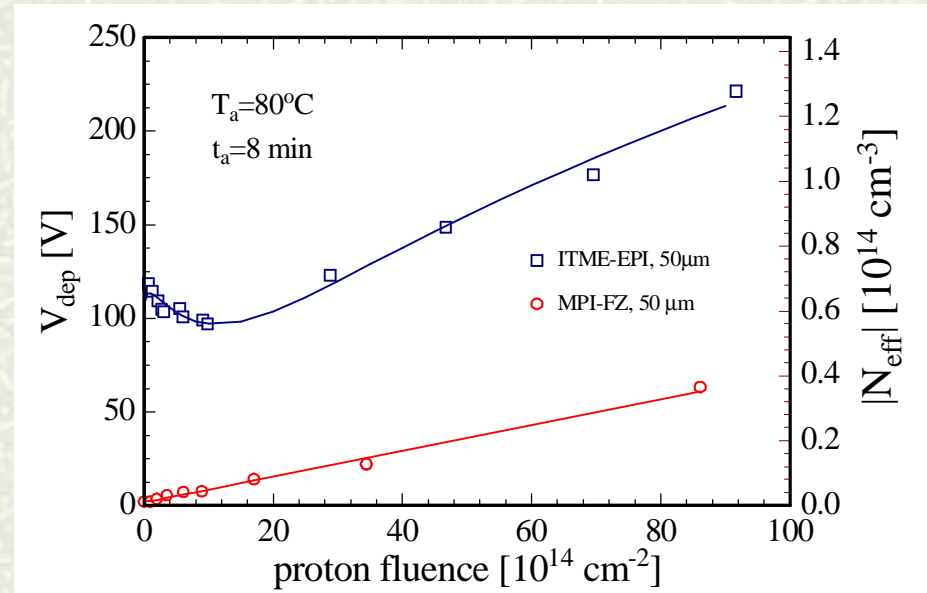
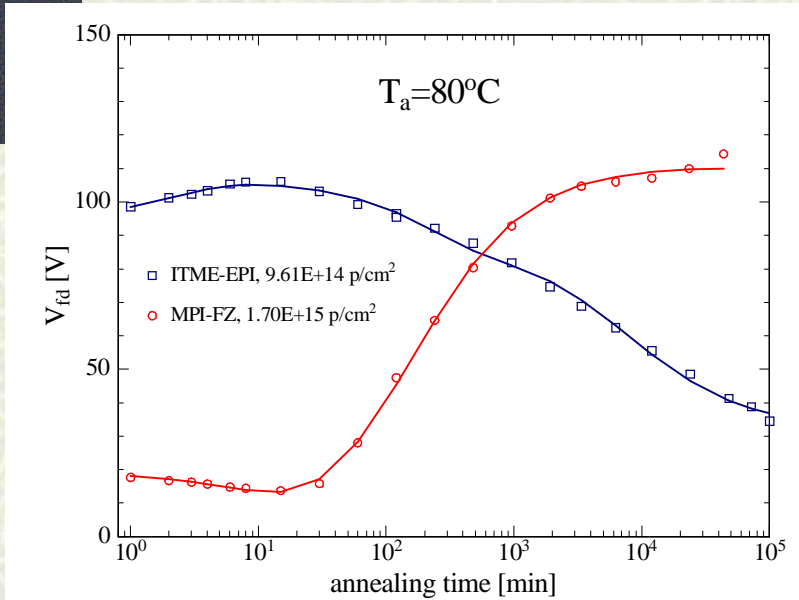
Advantages

1. Thin detectors present moderate depletion voltages even if highly doped ($V_{\text{dep},0} = qW^2N_{\text{eff},0}/2\epsilon$), with the advantage that the Space Charge Sign Inversion (SCSI) effect of the active layer, if present, is moved to higher fluences.
2. The CZ substrate is the backside n^+ ohmic contact, which is not depleted due to the high Sb doping level and acts also as a mechanical support for the thin epitaxial detector.
3. Due to the high oxygen concentration in the CZ substrate ($[\text{O}] \approx 10^{18}\ \text{cm}^{-3}$), O diffuses into the epitaxial layer during the high temperature growth process improving the detector radiation hardness.

Thin detector radiation hardness: epitaxial vs thinned

(E. Fretwurst et al., 4th RD50 Workshop, <http://rd50.web.cern.ch/rd50/4th-workshop>)

20-24 GeV proton irradiation



FZ thinned
(type inverted to p) { short term → V_{dep} decrease
long term → V_{dep} increase
(predominant acceptor generation)

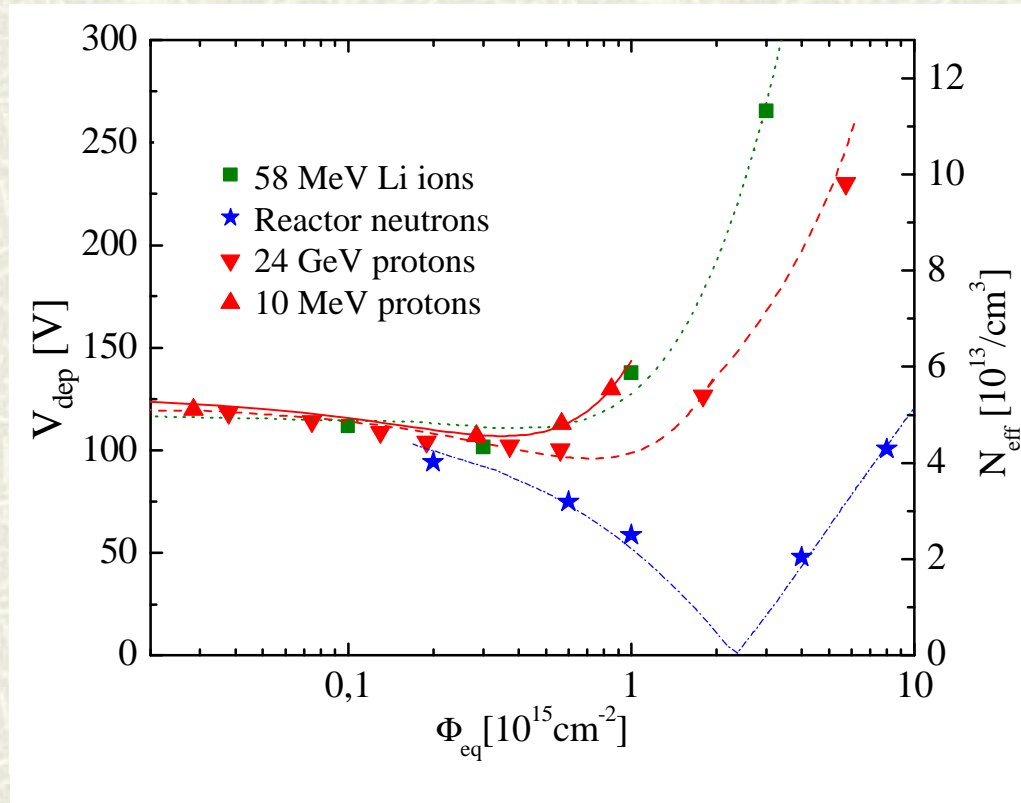
FZ thinned
(type inverted to p) { "low" [O]
predominant acceptor generation
during irradiation

Epitaxial
(no type inverted) { short term → V_{dep} increase
long term → V_{dep} decrease
(predominant acceptor generation)
no V_{dep} reverse annealing at RT!

Epitaxial
(no type inverted) { "high" [O]
predominant donor generation
during irradiation

Thin detector radiation hardness: epitaxial

(G. Lindstrom et al., 3rd RD50 Workshop, <http://rd50.web.cern.ch/rd50/3rd-workshop>)

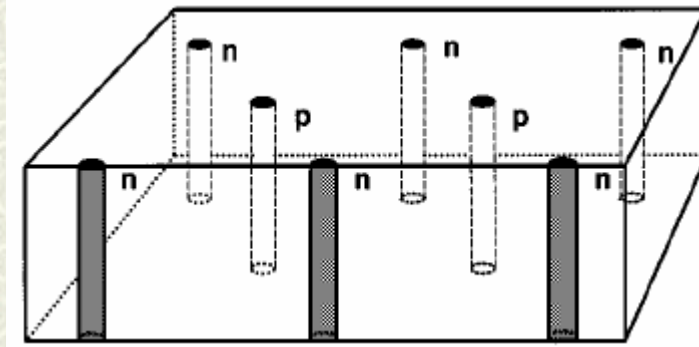


Epitaxial sensors can be **type-inverted by neutrons**

("low" [O] for cluster defects → predominant acceptor generation during irradiation)
but the high doping of the epitaxial layer moves the SCSI point to high fluences,
and V_{dep} is expected to be not higher than **125 V** at $F_{\text{eq}}=10^{16} \text{cm}^{-2}$,
so confirming the **extreme radiation hardness** of this technology.

3-D detectors

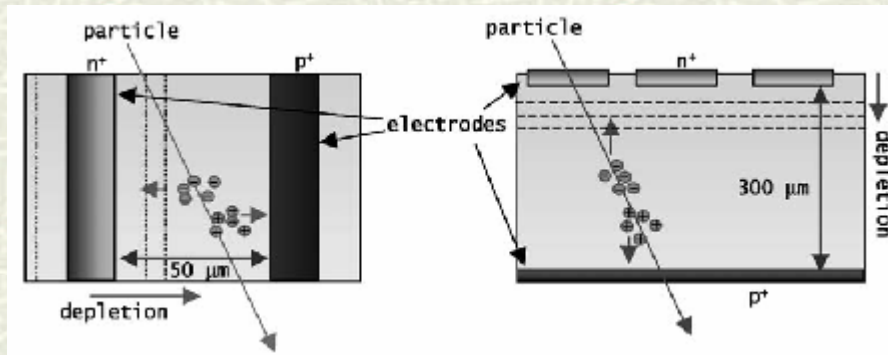
- Proposed by S.I. Parker, C.J. Kenney and J. Segal (NIM A 395 (1997) 328).
- Called 3-D because, in contrast to silicon planar technology, have **three dimensional (3-D) electrodes penetrating the silicon substrate**.
- Important researches are now under investigation by a collaboration (not in RD50) within Brunel Univ., Hawaii Univ., Stanford Univ., and CERN (see talk by A. Kok, tomorrow).



Picture taken from C.J. Kenney et al., IEEE TNS 48 (2001) 189.

Advantages:

- depletion thickness** depends on **p^+ and n^+ electrode distance**, not on the substrate thickness;
- lower collection length than planar technology;
- lower charge collection time than planar technology.

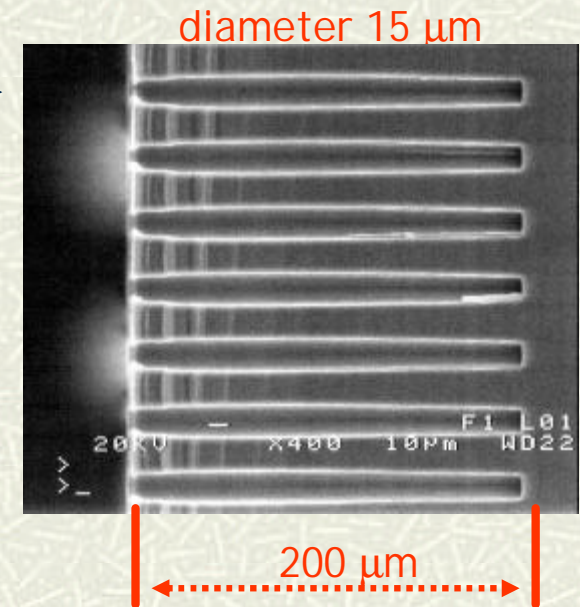


Picture taken from C. Da Via et al., NIM A 509 (2003) 86.

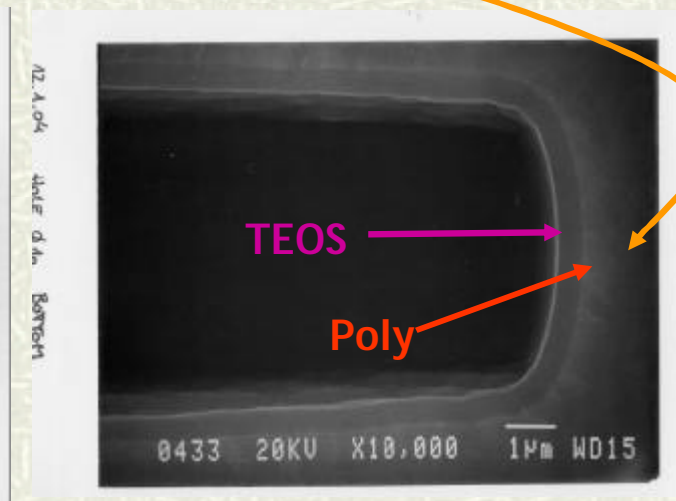
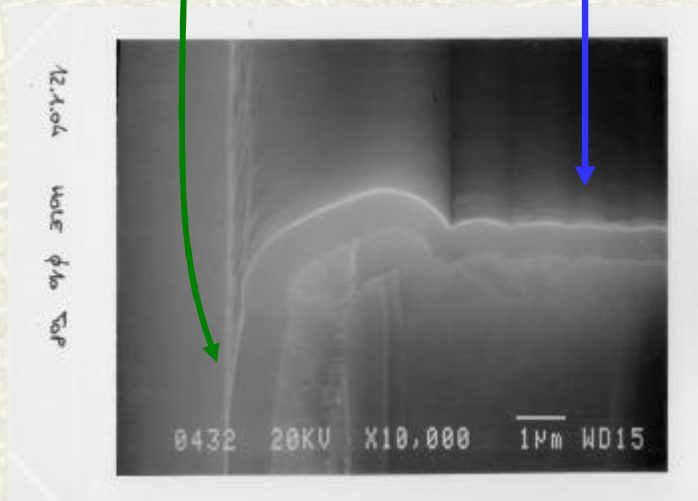
3-D detectors: going on activity in RD50

(M. Boscardin et al., 4th RD50 Workshop, <http://rd50.web.cern.ch/rd50/4th-workshop>)

- Detector masks: Glasgow University
- Deep reaction ion etching: CNM, Barcelona
- Detector processing: ITC-IRST, Trento



	Surface	Top	Bottom
Poly	1.05μm	0.8μm	0.7μm
TEOS	0.96μm	0.7μm	0.6 μm



Semi-3D detectors

(see talk by G. Kramberger, tomorrow)

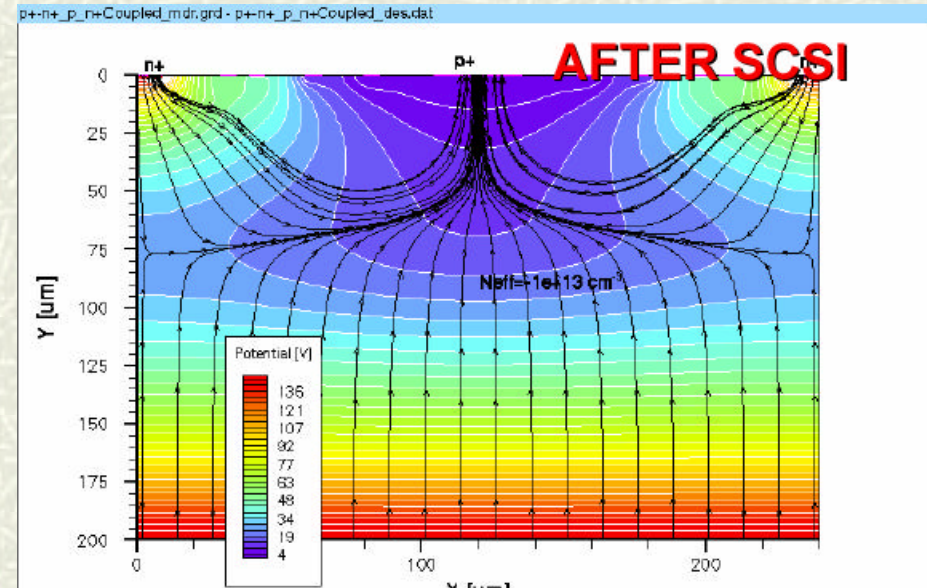
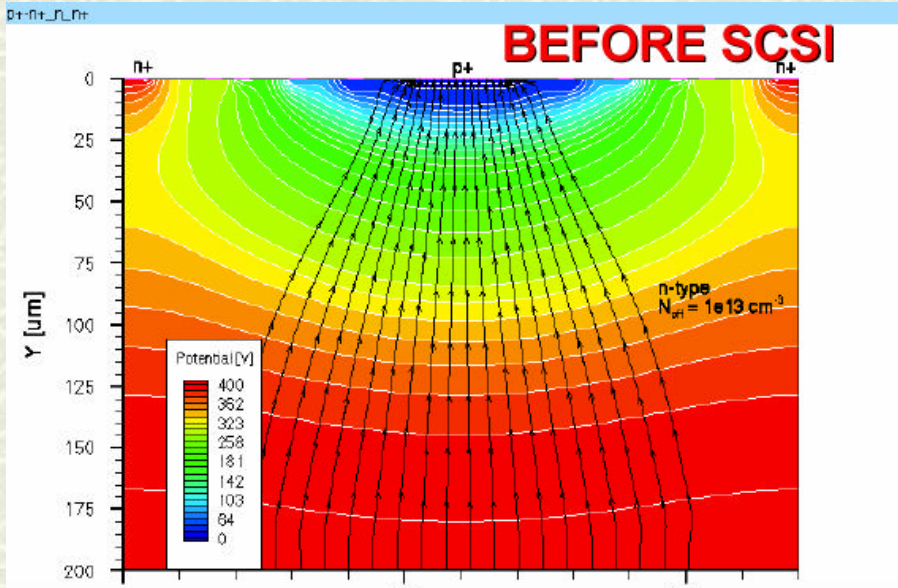
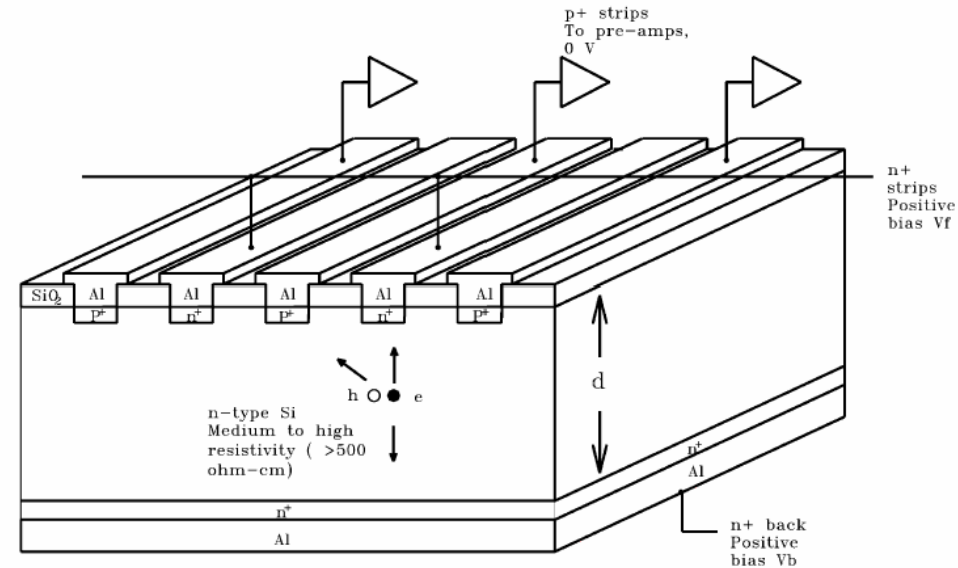
Proposed by Z. Li (NIM A 478 (2002) 303).
Single-side detectors with alternative p- and n- strips on the front side.

Advantages:

1. Single-side detector process.
2. After SCSI, the depletion occurs from both sides reducing the depletion voltage by factor 2.5.

Under investigation:

Complex electric field distribution before and after SCSI.



(Z. Li and D. Bortoletto, 4th RD50 Workshop, <http://rd50.web.cern.ch/rd50/4th-workshop>)

Stripixel detectors

Proposed by Z. Li (NIM A 518 (2004) 738).

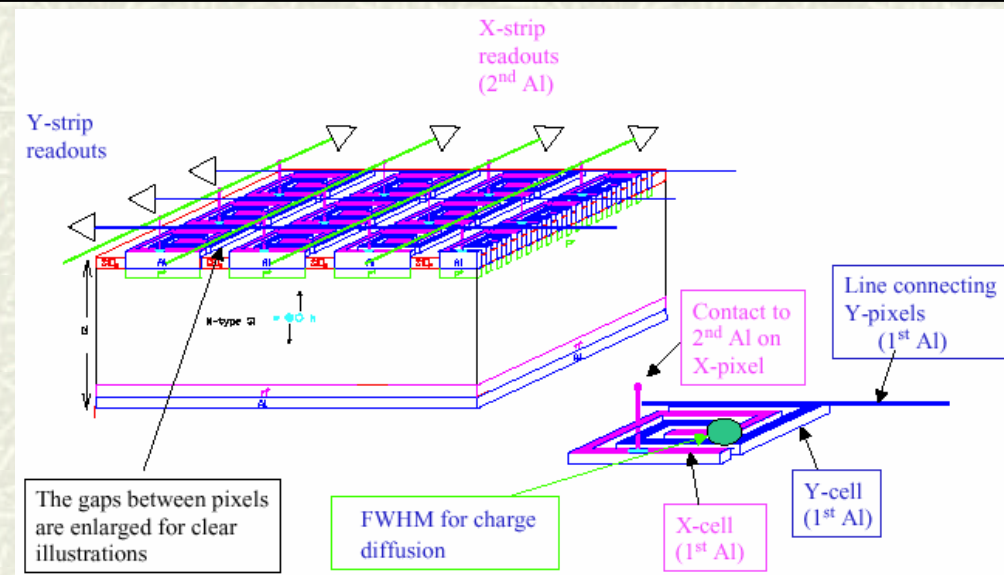
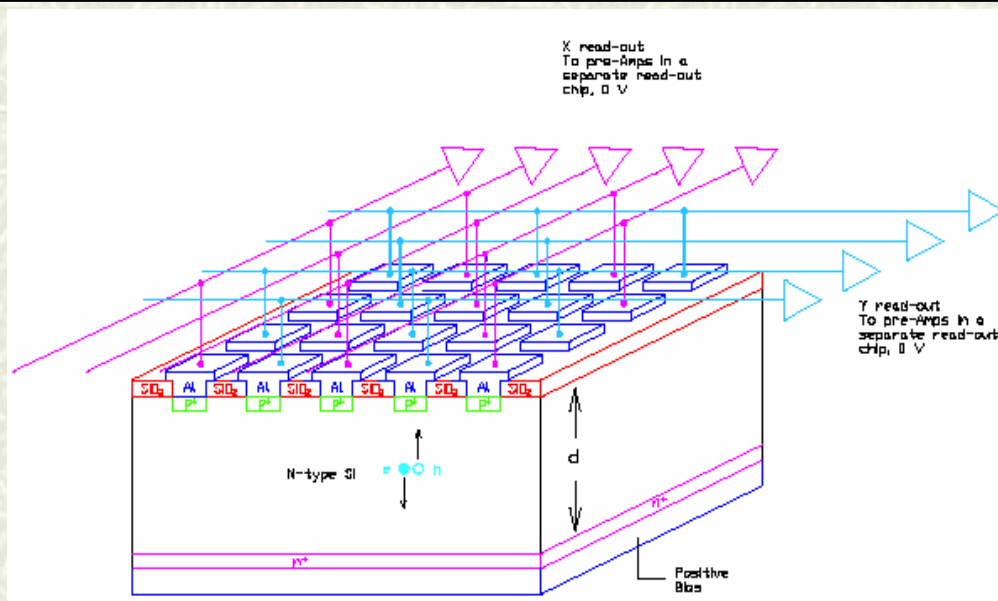
Pixel electrodes arranged in a projective X-Y readout.

Characteristics:

1. Projective readout of double-sided **strip** detectors minimizing the read-out channels;
2. Two-dimensional position resolution of **pixel** electrode geometry;
3. Single-side detector process with double metal technology;
4. Key parameter: standard deviation of the collected charge distribution: χ ($\approx 10 \mu\text{m}$).

- Individual pixels alternatively connected to X- and Y- read-out.
- Charge must be collected at least by two pixels.
- Key condition: $\chi \geq \text{pitch}$
- Resolution can be better than pitch.

- Each pixel is divided in two parts (X- and Y-cell).
- Charge must be collected at least by one X- and by one Y-cell.
- Key condition: $\chi \geq \text{interleaved distance between X- and Y- cells}$
- If $\text{pitch} > \chi$ the resolution is fixed by the pitch.



Alternative to macro-pixel detectors in the S-LHC upgrade between 15 cm and 60 cm?

n^+ -p detectors on DOFZ substrate

(G. Casse et al., NIM A 485 (2002) 153 and Proc. of the 10th VCI, Vienna, 16-21 Feb. 2004)

1. CCE(V) is improved if the read-out is at the high electric field contact: n^+ -p detectors (no SCS) **better than** p^+ -n sensors after SCS.
2. DOFZ p-type substrates are expected to be **more radiation hard** than FZ p-type Si.

Miniature n^+ -p microstrip detectors on DOFZ substrate

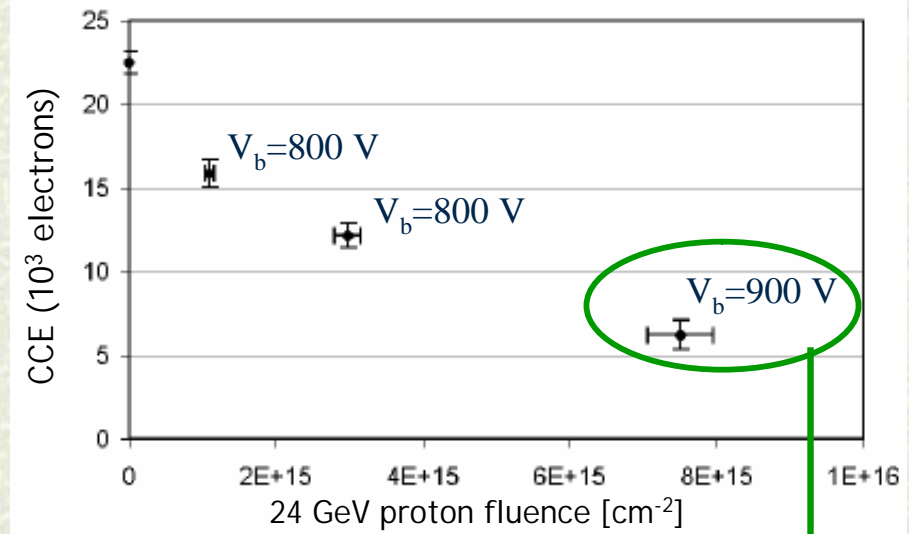
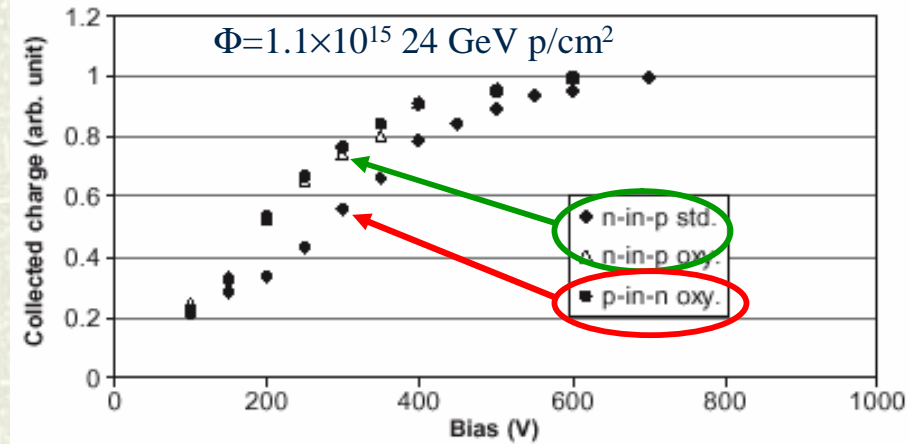
Area: $1 \times 1 \text{ cm}^2$

Thickness: $280 \text{ }\mu\text{m}$

Number of strips: 100

Read-out: SCT128 chip at 40 MHz

Source for CCE: ^{106}Ru



Charge, collected at 900 V bias after $7.5 \times 10^{15} \text{ 24-GeV p/cm}^2$ ($5 \times 10^{15} \text{ 1-MeV equivalent neutrons/cm}^2$) for **DOFZ p-type detector**, is **6500 electrons** (corresponding to the charge deposited in a $90 \text{ }\mu\text{m}$ thick un-irradiated silicon sensor).

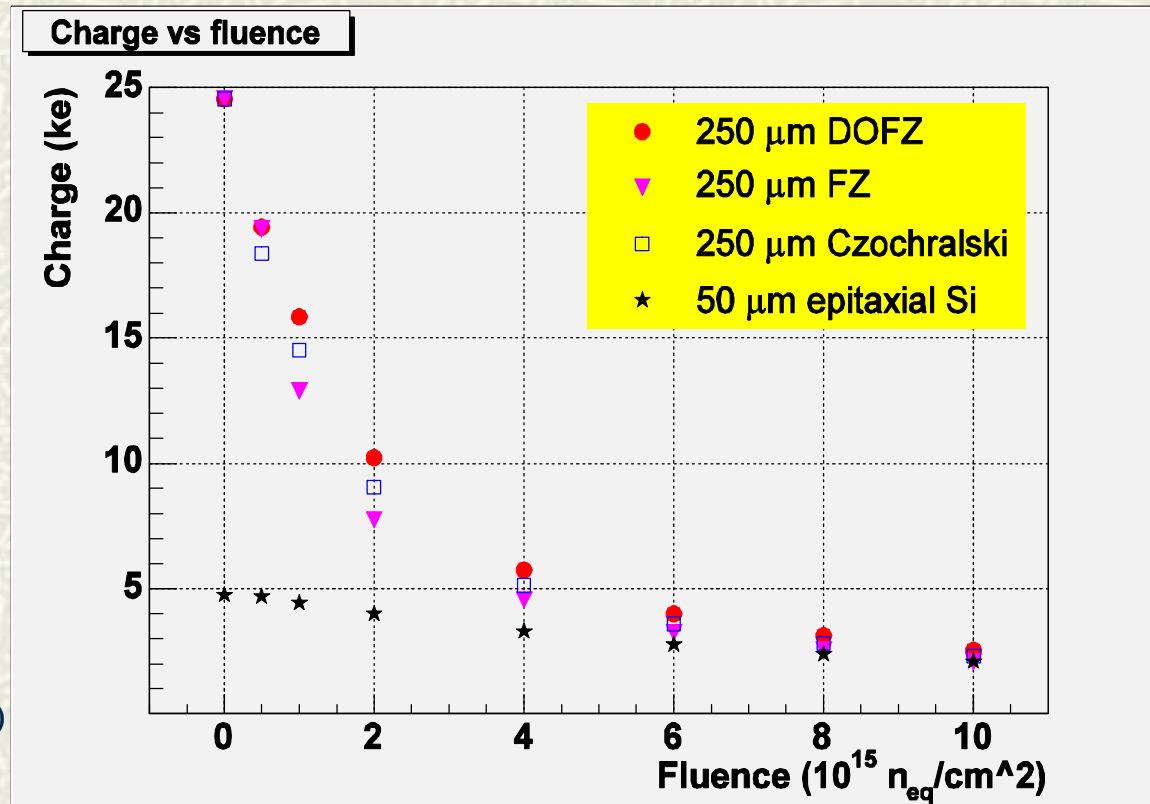
CCE simulations of pixel detectors

(T. Lari, Proc. of the 10th VCI, Vienna, 16-21 Feb. 2004)

Hypothesis:

1. Pixel dimensions: $70 \times 70 \mu\text{m}^2$ to cope with increased track density at SLHC.
2. $T = -10 \text{ }^\circ\text{C}$.
3. Read-out at the high electric field side:
 - n-side for FZ and DOFZ (type inverted);
 - p-side for Cz and Epitaxial (no type inverted).
4. V_{bias} : 600 V for FZ, DOFZ and CZ;
150 V for Epitaxial.

(see talks by T. Lari and G. Kramberger, tomorrow)



$10^{15} n_{\text{eq}}/\text{cm}^2$ fluence:

- DOFZ better than FZ when the latter is no longer fully depleted at 600 V.
- DOFZ (n-side read-out) slightly better than CZ (p-side read-out).
- Epitaxial signal very low (because of thin sensor).

$10^{16} n_{\text{eq}}/\text{cm}^2$ fluence:

- All detectors are similar (trapping dominant).

CCE in SiC and GaN

(A. Blue et al., 4th RD50 Workshop, <http://rd50.web.cern.ch/rd50/4th-workshop/>)

Material	Unirradiated CCE	Irradiated CCE
GaAs	100 % (MIPS) [2]	50 % (2×10^{14} 24 GeV protons/cm ²) [2]
SiC (100 μ m bulk V doped) **	60 % (5.486 Am^{241} alpha) [3]	50 % (10^{13} 300 MeV/c pions/cm ²) [3]
SiC (epi layer 30 μ m)	90 % (5.486 Am^{241} alpha) [4]	60 % (10^{14} 24 GeV/c protons/cm ²) [5]
Diamond	24 % (Mips) [6]	18 % (10^{15} 300 MeV/c pions/cm ²) [6]
GaN	95 % (5.486 Am^{241} alpha)	77 % (10^{14} 1 MeV neutrons/cm ²) 10% (10^{15} 1MeV neutrons/cm ²) 5% (10^{16} 1MeV neutrons/cm ²)

Si assumed to have 100 % CCE for all radiation types before irradiation

** 10^{18} cm^{-3} Vanadium (V) doped SiC maximum CCE 60 % [7]

[2] U. Biggeri et al, 'Noise behaviour of semi-insulating GaAs particle detectors before and after proton irradiation', Nucl. Phys. B (Proc. Suppl.) 78 (1999), 527- 532

[3] W. Cunningham et al, 'Performance of irradiated bulk SiC detectors', Nucl.Instr.and Meth. A 509 (2003), 127- 131

[4] G. Verzellezi et al, 'Investigation on the charge collection properties of a 4H-SiC Schottky diode detector', Nucl.Instr.and Meth. A 476 (2002), 717- 721

[5] F. Nava et al, 'Radiation tolerance of epitaxial silicon carbide detectors for electrons, protons and gamma-rays', Nucl.Instr.and Meth. A 505 (2003), 645- 655

[6] W. Adam et al, 'Radiation tolerance of CVD diamond detectors for pions and protons', Nucl.Instr.and Meth. A 476 (2002), 686- 693

Summary

General considerations:


1. **Leakage current** can be limited only by **decreasing temperature** ($\times 2$ every 7.5 K);
- 2a. **Charge collection** at the S-LHC fluences ($\geq 4\text{-}6 \times 10^{15} \text{ cm}^{-2}$) is **limited by carrier mean free path** and for planar technologies is less dependent on the detector thickness W .
- 2b. Benefits from **W decrease**: 1) $I_{\text{leak}} \propto W$; B) $V_{\text{dep}} \propto N_{\text{eff}} \cdot W^2$; C) $N_{\text{eff},0} \propto V_{\text{dep},0} / W^2$
3. **High [O]** required for limiting V_{dep} after irradiation thanks to **donor generation** (BD center) and **mitigation** of the **acceptor generation** (VO and V_2O or V_2 related defects are competitive processes): interesting results for **MCZ** (no SCSi with γ -rays), **CZ** (no SCSi with high energy charge hadrons), and **Epitaxial on CZ** (no reverse annealing for high energy charge hadrons);

Different technologies are under investigation in RD50:

1. Experimental data on different technologies are fundamental inputs for **devices simulations** in order **to determine** the **W**, **[O]** and **$N_{\text{eff},0}$** values **for the LHC upgrade**. W can be decreased accordingly to the maximum Φ and CCE required.
2. **CZ** and **MCZ** take advantage from higher [O] than FZ and DOFZ.
2. **Thinned devices** (50 μm) take advantage from $V_{\text{dep}} \propto W^2$, but small area sensors.
3. **Epitaxial** (50 μm) **on CZ** takes advantage from $V_{\text{dep}} \propto W^2$, high [O] and high $N_{\text{eff},0}$ (SCSi postponed), large area sensors. Possible to increase the thickness to 100 μm to increase CCE.

Different detector layouts are under investigation in RD50:

1. **3-D** (V_{dep} depends on the p-n electrode distance not on W), **Semi 3-D** (V_{dep} lower by a factor 2.5, but complex electric field), **Stripixel** (Single-side detector process with double metal technology for two-dimensional read-out, alternative to macro-pixels).



More material on the RD50 WEB site:
<http://rd50.web.cern.ch/rd50/>